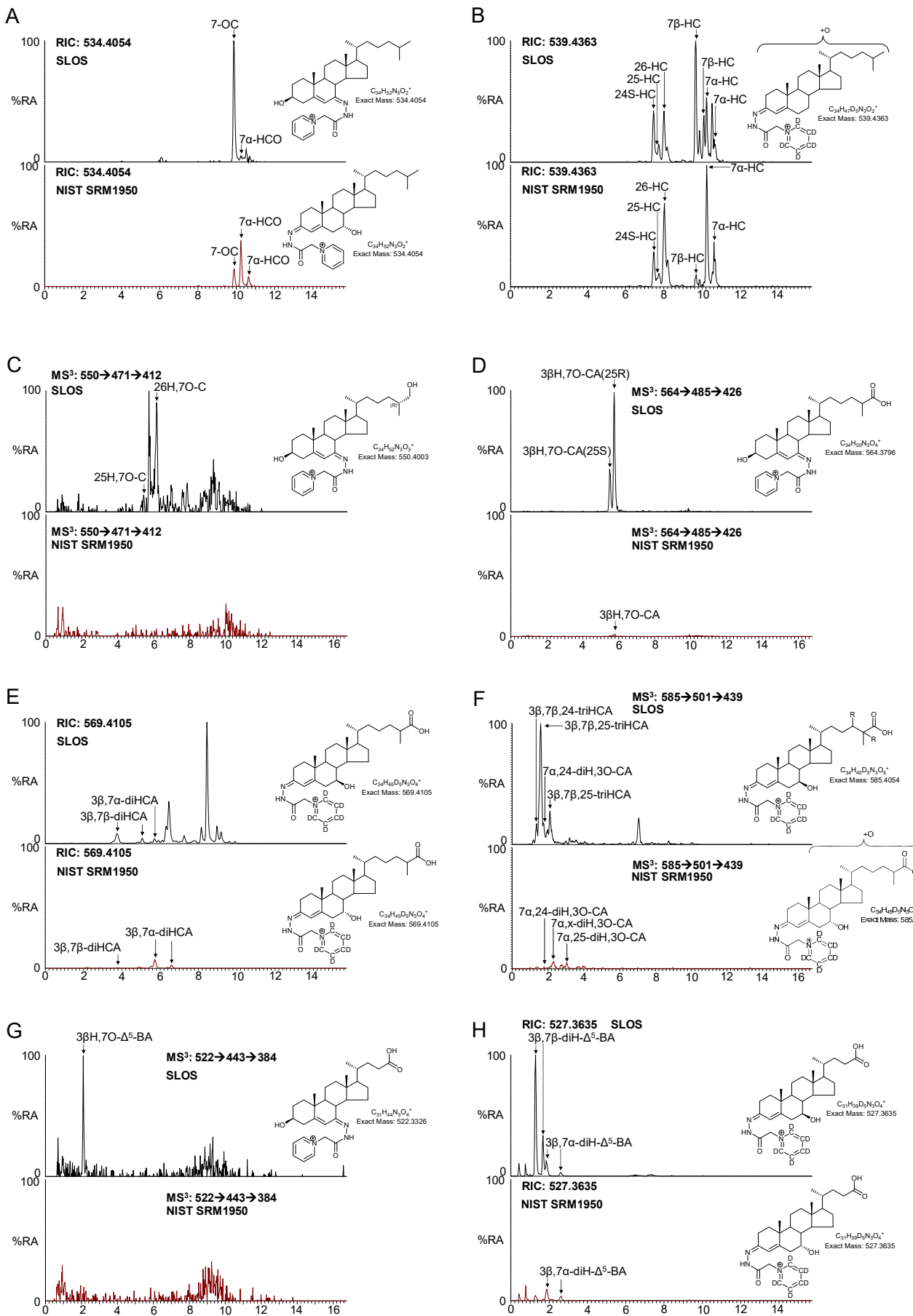


Figure S1. Principles of charge-tagging exemplified for 3 β ,7 β -dihydroxy- Δ^5 -BA and 3 β H,7O- Δ^5 -BA.



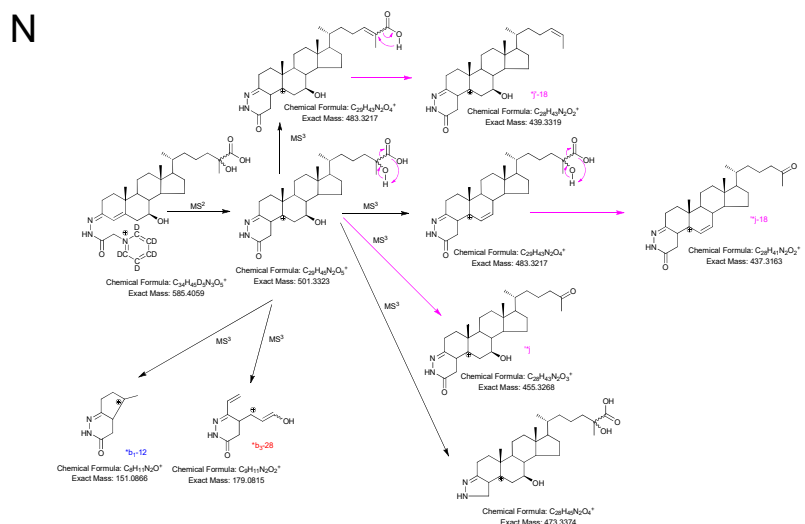
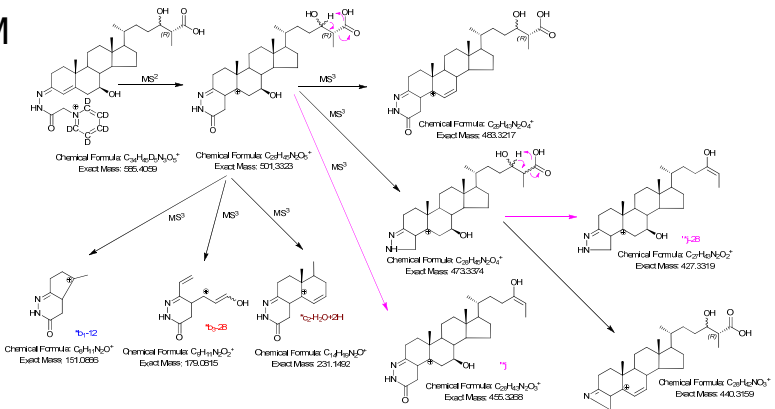
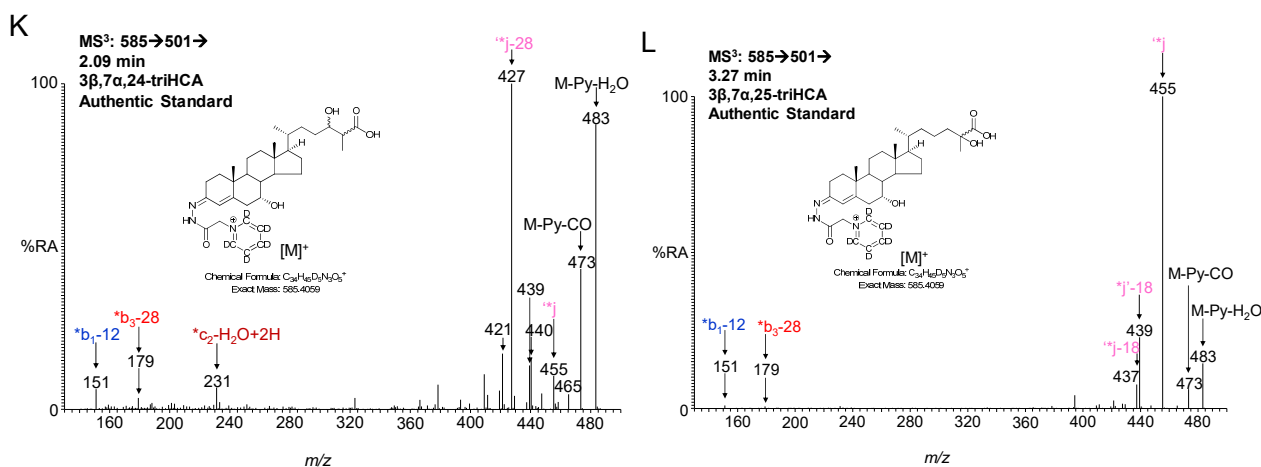
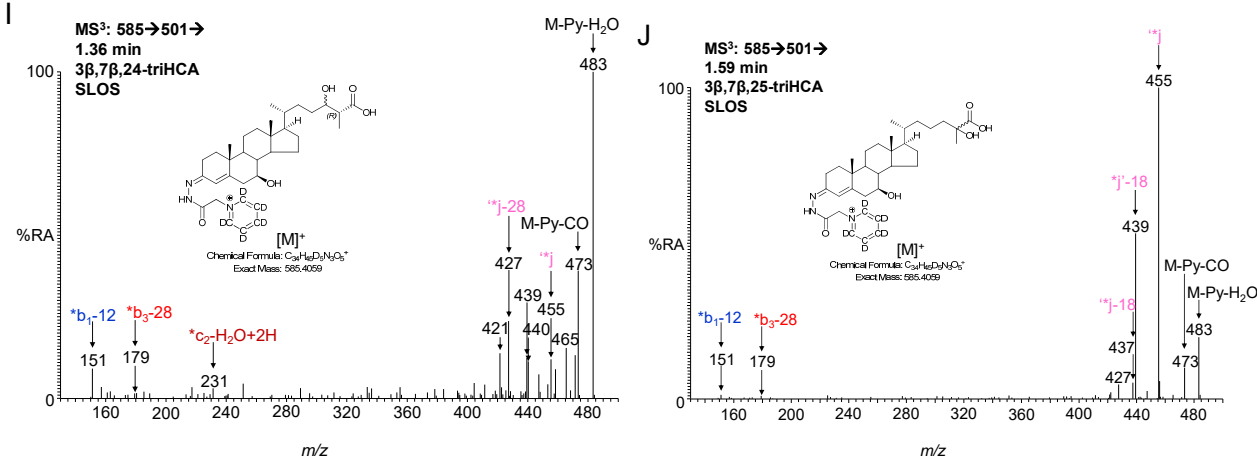


Figure S2. LC-MS(MS^n) analysis of oxysterols, including C₂₄ and C₂₇ acids, in plasma. Data was generated on a hybrid LIT-Orbitrap. Samples prepared in the presence of cholesterol oxidase utilised the [²H₅]GP derivatisation reagent resulting in odd *m/z* molecular ions, samples prepared in the absence of cholesterol oxidase utilised [²H₀]GP reagent resulting in even *m/z* molecular ions. Upper panels are for an SLOS plasma sample, lower panels are for the NIST SRM 1950 (1). Upper and lower panels are shown on the same y-axis. GP derivatives give *syn* and *anti* conformers, which may or may not be resolved. (A) Reconstructed ion chromatogram (RIC) of *m/z* 534.4054 ± 10 ppm corresponding to 7-OC and 7α-hydroxycholest-4-en-3-one (7α-HCO). Samples were prepared in the absence of cholesterol oxidase. (B) RIC of *m/z* 539.4363 ± 10 ppm corresponding to monohydroxycholesterols (HC). Samples were prepared in the presence of cholesterol oxidase. (C) MS³ multiple reaction monitoring transition (MRM) 550→471→412 characteristic of 26H,7O-C. Samples were prepared in the absence of cholesterol oxidase. (D) MS³ MRM 564→485→426 characteristic of 3βH,7O-CA. Note, both 25R and 25S-epimers are resolved. Samples were prepared in the absence of cholesterol oxidase. (E) RIC of *m/z* 569.4105 ± 10 ppm corresponding to dihydroxycholestenoic acids (diHCA). Samples were prepared in the presence of cholesterol oxidase. (F) MS³ MRM 585→501→439 characteristic of the trihydroxycholestenoic acids (triHCA) 3β,7,24(or25)-triHCA. Samples were prepared in the presence of cholesterol oxidase. (G) MS³ MRM 522→443→384 characteristic of 3βH,7O-Δ⁵-BA. Samples were prepared in the absence of cholesterol oxidase. (H) RIC of *m/z* 527.3635 ± 10 ppm corresponding to dihydroxycholenic (diH-Δ⁵-BA) and hydroxyoxocholenic acids. Samples were prepared in the presence of cholesterol oxidase. MS³ ([M]⁺→[M-Py]⁺→) spectra of (I) 3β,7β,24-triHCA, (J) 3β,7β,25-triHCA, both from SLOS plasma, and authentic standards (K) 3β,7α,24-triHCA and (L) 3β,7α,25-triHCA. Fragmentation patterns of (M) 3β,7β,24-triHCA and (N) 3β,7β,25-triHCA. Details of the fragmentation pathways of 7-oxo compounds in (C), (D) and (G) can be found in reference (2).

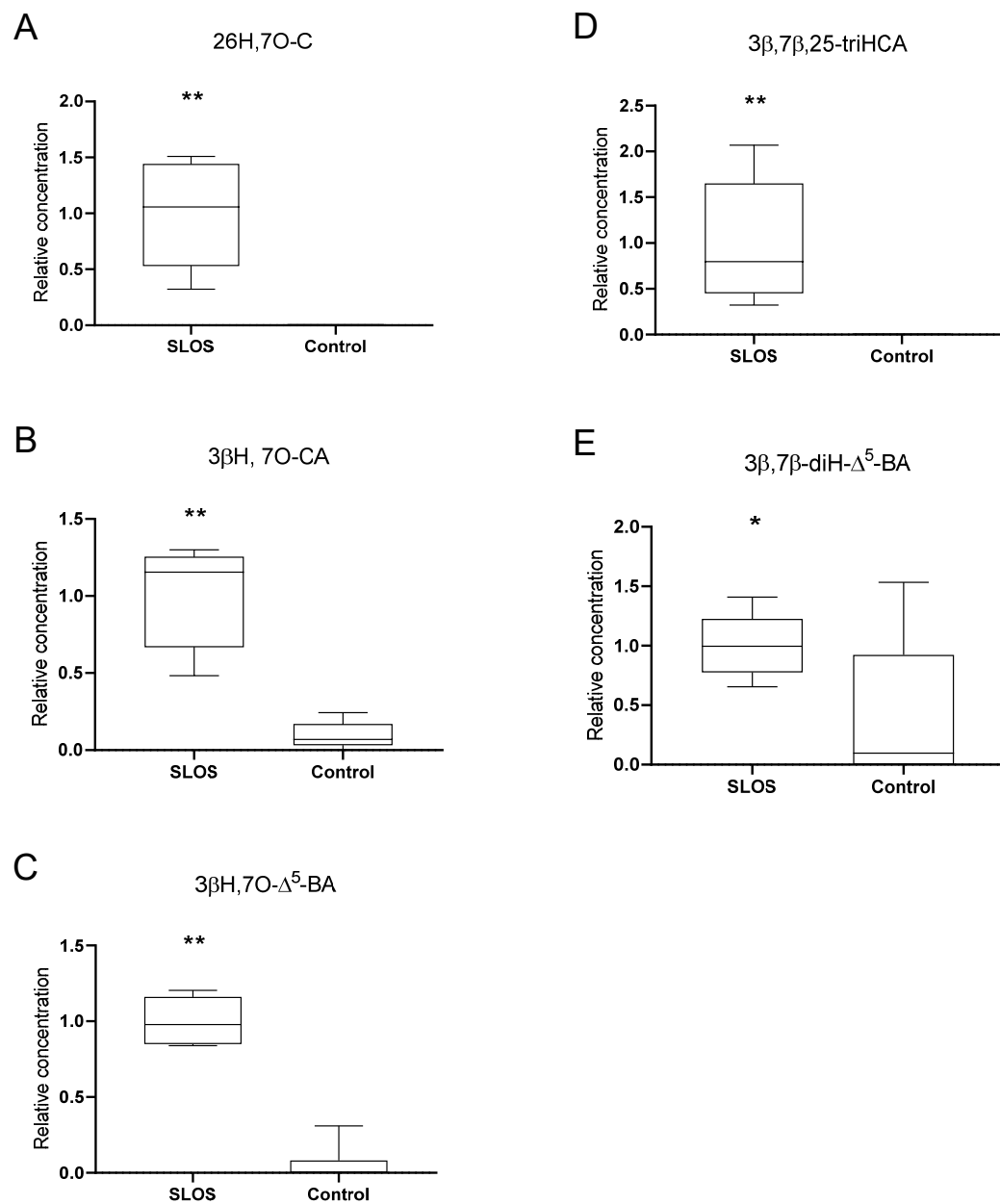


Figure S3. Relative concentrations of 26-hydroxy-7-oxocholesterol and 7 β -hydroxy- and 7-oxo- C₂₄ and C₂₇ acids in amniotic fluid from SLOS affected pregnancies (n = 5) and healthy pregnancies (n = 12). (A) 26H,7O-C. (B) 3 β H,7O-CA. (C) 3 β H,7O- Δ^5 -BA. (D) 3 β ,7 β ,25-triHCA. (E) 3 β ,7 β -diH- Δ^5 -BA. For each analyte relative concentrations were determined against [²H]₇24R/S-HC internal standard and normalised to the mean value for SLOS set to 1. Statistical comparisons are made as described in the caption to Figure 2.

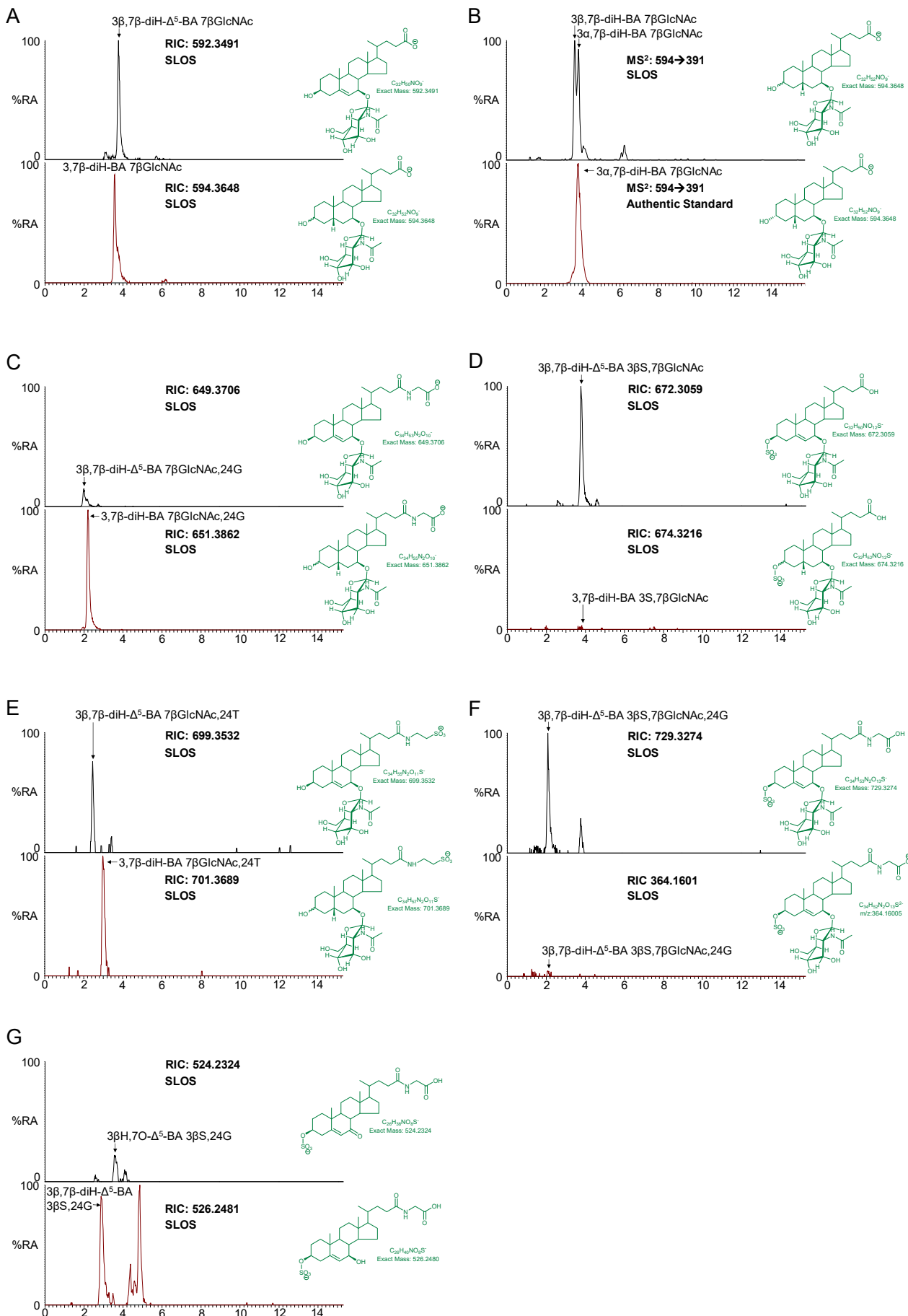


Figure S4. LC-MS(MS^n) analysis of GlcNAc conjugated bile acids in SLOS urine. Data was generated on a hybrid LIT-Orbitrap in the negative-ion mode. RIC \pm 10 ppm are of $[M-H]^-$ ions (unless stated otherwise). Upper and lower panels are shown on the same y-axis. (A) RIC of m/z 592.3491 (upper panel) and 594.3648 (lower panel) corresponding to $3\beta,7\beta$ -diH- Δ^5 -BA 7 β GlcNAc and $3,7\beta$ -diH-BA 7 β GlcNAc, respectively. (B) MS^2 MRM 594 \rightarrow 391 characteristic of $3,7\beta$ -diH-BA 7 β GlcNAc. The upper panel shows partial separation of $3\alpha,7\beta$ -diH-BA 7 β GlcNAc from the 3β -epimer in an SLOS sample. The lower panel shows $3\alpha,7\beta$ -diH-BA 7 β GlcNAc authentic standard. (C) RIC of m/z 649.3706 (upper panel) and m/z 651.3862 (lower panel) corresponding to $3\beta,7\beta$ -diH- Δ^5 -BA 7 β GlcNAc,24G and $3,7\beta$ -diH-BA 7 β GlcNAc,24G, respectively. (D) RIC of m/z 672.3059 (upper panel) and m/z 674.3216 (lower panel) corresponding to $3\beta,7\beta$ -diH- Δ^5 -BA 3 β S,7 β GlcNAc and $3,7\beta$ -diH-BA 3S,7 β GlcNAc, respectively. (E) RIC of m/z 699.3532 (upper panel) and m/z 701.3689 (lower panel) corresponding to $3\beta,7\beta$ -diH- Δ^5 -BA 7 β GlcNAc,24T and $3,7\beta$ -diH-BA 7 β GlcNAc,24T, respectively. (F) RIC of m/z 729.3274 (upper panel) and m/z 364.1601 (lower panel) corresponding to $3\beta,7\beta$ -diH- Δ^5 -BA 3 β S,7 β GlcNAc,24G as $[M-H]^-$ and $[M-2H]^{2-}$ ions, respectively. (G) RIC of m/z 524.2324 (upper panel) and m/z 526.2481 (lower panel) corresponding to 3β H,7O- Δ^5 -BA 3 β S,24G and $3\beta,7\beta$ -diH- Δ^5 -BA 3 β S,24G, respectively.

1. Quehenberger, O., A. M. Armando, A. H. Brown, S. B. Milne, D. S. Myers, A. H. Merrill, S. Bandyopadhyay, K. N. Jones, S. Kelly, R. L. Shaner, C. M. Sullards, E. Wang, R. C. Murphy, R. M. Barkley, T. J. Leiker, C. R. Raetz, Z. Guan, G. M. Laird, D. A. Six, D. W. Russell, J. G. McDonald, S. Subramaniam, E. Fahy, and E. A. Dennis. 2010. Lipidomics reveals a remarkable diversity of lipids in human plasma. *J Lipid Res* **51**: 3299-3305.
2. Griffiths, W. J., I. Gilmore, E. Yutuc, J. Abdel-Khalik, P. J. Crick, T. Hearn, A. Dickson, B. W. Bigger, T. H. Wu, A. Goenka, A. Ghosh, S. A. Jones, and Y. Wang. 2018. Identification of unusual oxysterols and bile acids with 7-oxo or 3β ,5 α ,6 β -trihydroxy functions in human plasma by charge-tagging mass spectrometry with multistage fragmentation. *J Lipid Res* **59**: 1058-1070.